MCB
Journals.ASM.org

Hippo Signaling Regulates Pancreas Development through Inactivation of Yap

Nicholas M. George,[a,b] Caroline E. Day,[a,b] Brian P. Boerner,[b,c] Randy L. Johnson,[d] and Nora E. Sarvetnick[a,b]

Department of Surgery, University of Nebraska Medical Center, Omaha, Nebraska, USA[a]; Regenerative Medicine Project, University of Nebraska Medical Center, Omaha, Nebraska, USA[b]; Department of Internal Medicine, University of Nebraska Medical Center, Omaha, Nebraska, USA[c]; and Department of Biochemistry and Molecular Biology, M. D. Anderson Cancer Center, Houston, Texas, USA[d]

The mammalian pancreas is required for normal metabolism, with defects in this vital organ commonly observed in cancer and diabetes. Development must therefore be tightly controlled in order to produce a pancreas of correct size, cell type composition, and physiologic function. Through negative regulation of Yap-dependent proliferation, the Hippo kinase cascade is a critical regulator of organ growth. To investigate the role of Hippo signaling in pancreas biology, we deleted Hippo pathway components in the developing mouse pancreas. Unexpectedly, the pancreas from Hippo-deficient offspring was reduced in size, with defects evident throughout the organ. Increases in the dephosphorylated nuclear form of Yap are apparent throughout the exocrine compartment and correlate with increases in levels of cell proliferation. However, the mutant exocrine tissue displays extensive disorganization leading to pancreatitis-like autodigestion. Interestingly, our results suggest that Hippo signaling does not directly regulate the pancreas endocrine compartment as Yap expression is lost following endocrine specification through a Hippo-independent mechanism. Altogether, our results demonstrate that Hippo signaling plays a crucial role in pancreas development and provide novel routes to a better understanding of pathological conditions that affect this organ.

First identified in *Drosophila* and highly conserved in mammals, the Hippo pathway consists of a series of kinases thought to be regulated by cell-cell contact (7, 19, 33). This pathway is activated by undefined signals most likely emanating from the cell surface, which leads to activation of the redundant mammalian Ste20-like kinases Mst1 and Mst2 (Mst1/2). Through Mst1/2 association with its adapter protein Salvador-1, Mst1/2 phosphorylates and thereby activates large tumor suppressor 1 and 2 (Lats1 and Lats2), which in turn phosphorylate the transcriptional coactivator, Yes-associated protein (Yap) (31). Upon phosphorylation, Yap is sequestered within the cytoplasm through association with 14-3-3 family members and subsequently degraded in a proteasome-dependent manner, resulting in the termination of its biological effects (29, 34). In the absence of phosphorylation, Yap exists in the nucleus where it stimulates expression of genes required for cell proliferation, such as connective tissue growth factor and the epidermal growth factor (EGF) family member amphiregulin (29, 32). Thus, cell and tissue growth are restricted by an activated Hippo kinase cascade.

The mammalian pancreas is a dual-function organ critical for the regulation of basic metabolism. In the mouse, development of the pancreas is divided into two stages, commonly denoted as the primary and secondary transitions (21). Occurring between embryonic days 9.5 and 12.5 (E9.5 and E12.5, respectively), the primary transition refers to the morphogenetic changes that occur within the pancreatic epithelium, resulting in finger-like projections present throughout the mesenchyme. At the onset of the primary transition, cells are marked by expression of the homeobox transcription factor, Pdx1. Absolute numbers of Pdx1-expressing progenitor cells have been shown to govern final pancreas size and give rise to all three types of pancreas tissue (e.g., ducts, acinar, and endocrine cells) (9, 27). The secondary transition, occurring between E13.5 and E16.5, is characterized by robust proliferation and differentiation throughout the pancreas epithelium. During this period, the acinar cell compartment, which is dependent on expression of the basic helix-loop-helix (bHLH) transcription factor, Ptf1a, expands in mass via mitosis, while endocrine progenitor cells, which are dependent on expression of the bHLH transcription factor Ngn3, delaminate from the Sox9-expressing ductal epithelium (8, 16). Ngn3-dependent endocrine specification is commonly associated with these cells becoming mitotically quiescent in route to terminal differentiation (6, 9, 20).

Although the factors required for specifying individual pancreas cell subsets are fairly well known, less is known about the signaling pathways responsible for regulating proliferation and survival of these populations. To date, Wnt/β-catenin and phosphoinositide 3-kinase (PI3K) signaling have been shown to play significant roles. Stabilization of β-catenin or knockout of its endogenous inhibitor, adenomatous polyposis coli (APC), results in robust acinar cell proliferation and generation of a pancreas twice the normal size (11, 28). On the other hand, loss of PTEN, the main negative regulator of PI3K signaling, leads to proliferation of terminal duct cells and gradual replacement of acinar tissue with metaplastic ducts (26). Molecular genetic analysis of additional biochemical pathways, for example, those involved in organ size determination, may provide further insight into the mechanisms governing pancreas development.

In the present study, we investigated the physiological role of Hippo signaling in pancreas biology by genetically deleting the critical Hippo signaling mediators Mst1/2 at the onset of pancreas

Received 1 August 2012 **Returned for modification** 23 August 2012
Accepted 5 October 2012
Published ahead of print 15 October 2012
Address correspondence to Nicholas M. George, nmgeorge@unmc.edu.
Supplemental material for this article may be found at http://mcb.asm.org/.

doi:10.1128/MCB.01034-12

development. Our experiments establish that Hippo signaling becomes functionally active during the secondary transition and plays a crucial role in determining overall pancreas architecture, likely through downregulation of Yap-dependent cell proliferation. Our analysis demonstrated tissue disorganization throughout the mutant pancreas, with widespread presence of exocrine transitional structures, regions consisting of a mixed acinar and ductal phenotype. Most likely the result of exocrine disorganization, pancreatitis-like autodigestion was prominent throughout the Hippo knockout pancreas. Lastly, we found that very early in pancreas development, expression of Yap is turned off following specification of endocrine fate, potentially explaining the poor proliferation capacity displayed by these cells. Taken together, these results define a fundamental role for Hippo signaling during pancreas development, determining overall pancreas architecture and physiological function.

MATERIALS AND METHODS

Breeding of pancreas-specific Hippo knockout mice. Generation of floxed Mst1/2 and Pdx1-Cre strains is presented elsewhere (12, 18). The Mst1/2$^{lox/lox}$ strain was crossed with the Pdx1-Cre strain to produce heterozygous offspring, which, in turn, were backcrossed with homozygous Mst1/2$^{lox/lox}$ to produce Mst1/2 double-knockout offspring at a frequency of 0.125. Control mice for all experiments were those lacking Cre recombinase expression. All breeding and experimental procedures were approved by the University of Nebraska Medical Center. For blood glucose measurements, anesthetized animals were restrained, and the tail was cut with a sterile razor blade. A single drop of blood was then read using a glucometer (One Touch Ultra; LifeScan Inc., Milpitas, CA). Glucose tolerance tests (1 U/gram of body weight) were performed on mice following overnight fasting. For embryo isolation, timed mating was prepared by pairing virgin females with proven breeder males prior to the end of the daily light schedule. Breeders were separated the following morning (day E0.5) and sacrificed thereafter (E12.5 or E16.5). Embryo proliferation studies were completed by intraperitoneally (i.p.) injecting the pregnant mother with bromodeoxyuridine (BrdU) (20 mM stock; 5 ml/kg of body weight) 2 h prior to sacrifice. Unless otherwise noted, all adult offspring used in experiments were 6 weeks old.

Tissue processing. Mice were euthanized with isoflurane, and adult or embryonic tissues were dissected into ice-cold phosphate-buffered saline (PBS). For proliferation studies in adult mice, 0.8 mg/ml bromodeoxyuridine (BrdU) (Sigma-Aldrich, St. Louis, MO) was added to the microisolator drinking water 48 h prior to sacrifice. Excised pancreas tissue was fixed in 10% formalin in PBS overnight at room temperature and then processed for paraffin embedding. Sections were cut at 4 μm and then used for hematoxylin and eosin (H&E) or immunostaining.

Immunostaining. Primary and secondary antibodies used in this study are provided in Table S1 in the supplemental material. The tyramide signal amplification (TSA) reagent was from Perkin Elmer Inc. (Waltham, MA) and was used only with Hes1 antibody. All photomicrograph images are representative of at least three samples of the indicated genotype and age.

For immunohistochemistry, sections were dewaxed and rehydrated, and these steps were followed by antigen retrieval in 10 mM citrate (pH 6.0). Endogenous peroxidase activity was then quenched with 3% H_2O_2 in methanol. Following washes in PBS, sections were blocked with 3% goat serum in PBS. Primary and secondary (biotin-labeled) antibody incubations were followed by VectaStain ABC reagent (Vector Laboratories, Burlingame, CA) and then development with DAB (diaminobenzidine) Plus reagent (Fisher Scientific, Waltham MA). Hematoxylin (Fisher Scientific) costaining was completed, followed by mounting with CytoSeal XYL (Fisher Scientific). PO_4-S6 and PO_4-4E-BP1 (where 4E-BP1 is eukaryotic translation initiation factor 4E binding protein 1) staining utilized methyl green counterstaining in place of hematoxylin. CD3 and Mac3 staining was performed similarly, except that ImmPACT VIP reagent was used to develop signal, and methyl green was used to counterstain (both from Vector Laboratories). Apoptotic cells were detected using an *In situ* Cell Death Detection Kit (Roche, Indianapolis, IN) according to the manufacturer's protocol. For quantitation of proliferating cells, three independent areas per sample were photographed and counted by blinded eye.

Immunofluorescent staining was performed similarly to immunohistochemistry with the omission of the peroxidase quenching step. Additionally, the blocking solution consisted of 5% normal donkey serum (Jackson ImmunoResearch, West Grove, PA) in PBS. Costaining with Sox9 and Ptf1a required the use of ImmunoStain Enhancer according to the manufacturer-provided protocol (Fisher Scientific). Secondary antibodies were donkey antibody-Alexa Fluor 488 or 594 conjugates (Life Technologies, Carlsbad, CA). Slides were coverslipped with 4′,6-diamidino-2-phenylindole (DAPI)-containing VectaShield Hard-Set mounting medium (Vector Laboratories). All slides were observed and images were captured using an Axio Imager (Carl Zeiss, Oberkochen, Germany). Image overlay was completed using Photoshop CS5 software (Adobe Systems Inc., San Jose, CA).

Western blot analysis. Six hundred microliters of EBC buffer (50 mM Tris, 120 mM NaCl, 0.5% NP-40, pH 7.4, containing complete protease and phosphatase inhibitors [Fisher Scientific]) was added to 50 to 100 mg of whole mouse pancreas and Dounce homogenized on ice. Homogenates were transferred to 1.5-ml Epi tubes and inverted for 30 min at 4°C, followed by centrifugation at 20,000 rpm at 4°C for 20 min. Total protein concentrations were normalized using the commercially available Bio-Rad assay. Protein samples were run on 10% SDS-PAGE gels, which was followed by transfer to nitrocellulose membranes. Primary antibodies (see Table S1 in the supplemental material) were incubated overnight at 4°C while peroxidase-conjugated secondary antibodies (Jackson ImmunoResearch) were incubated for 1 h at room temperature. All membranes were developed with enhanced chemiluminescence (ECL) reagents purchased from Fisher Scientific.

RESULTS

Expression pattern of Yap and activated Mst1/2 in the mammalian pancreas. The expression and cellular localization of Yap have previously been shown to overlap defined stem cell compartments in some tissues. For example, both the crypt cells of the intestine and the single-layered basal epidermal progenitors of the skin harbor readily detectible and nucleus-localized Yap (3, 4, 30). We used immunohistochemical analysis to determine which cell lineages in the mammalian pancreas express Yap. As shown in Fig. 1A and B, Yap is expressed throughout the embryonic day 12.5 (E12.5) mouse pancreas, as demonstrated by serial staining for Pdx1. Cells found within the acinus-destined "tip" region display robust Yap nuclear localization, whereas those found within the duct- and endocrine-fated "trunk" (green arrow) are either strongly Yap positive or, alternatively, devoid of Yap expression. While E12.5 is characterized by compartmentalization within the developing pancreas, the secondary transition (~E16.5) is characterized by massive cell proliferation and differentiation. As shown in Fig. 1C, Yap expression at E16.5 becomes gradually limited to prospective ductal and acinar regions. Interestingly, nuclear Yap expression remains high within the productal cells (yellow arrow), whereas acinus-fated cells demonstrate Yap immunoreactivity mostly within the cytoplasm (orange arrows). Strikingly, prospective endocrine cells lack detectible Yap expression (green arrows). Unlike the embryonic pancreas, the adult mouse pancreas displays a greatly reduced number of Yap-expressing cells (Fig. 1D). Ductal and terminal-duct centroacinar cells express the highest levels of Yap. Acinar cells display a weak

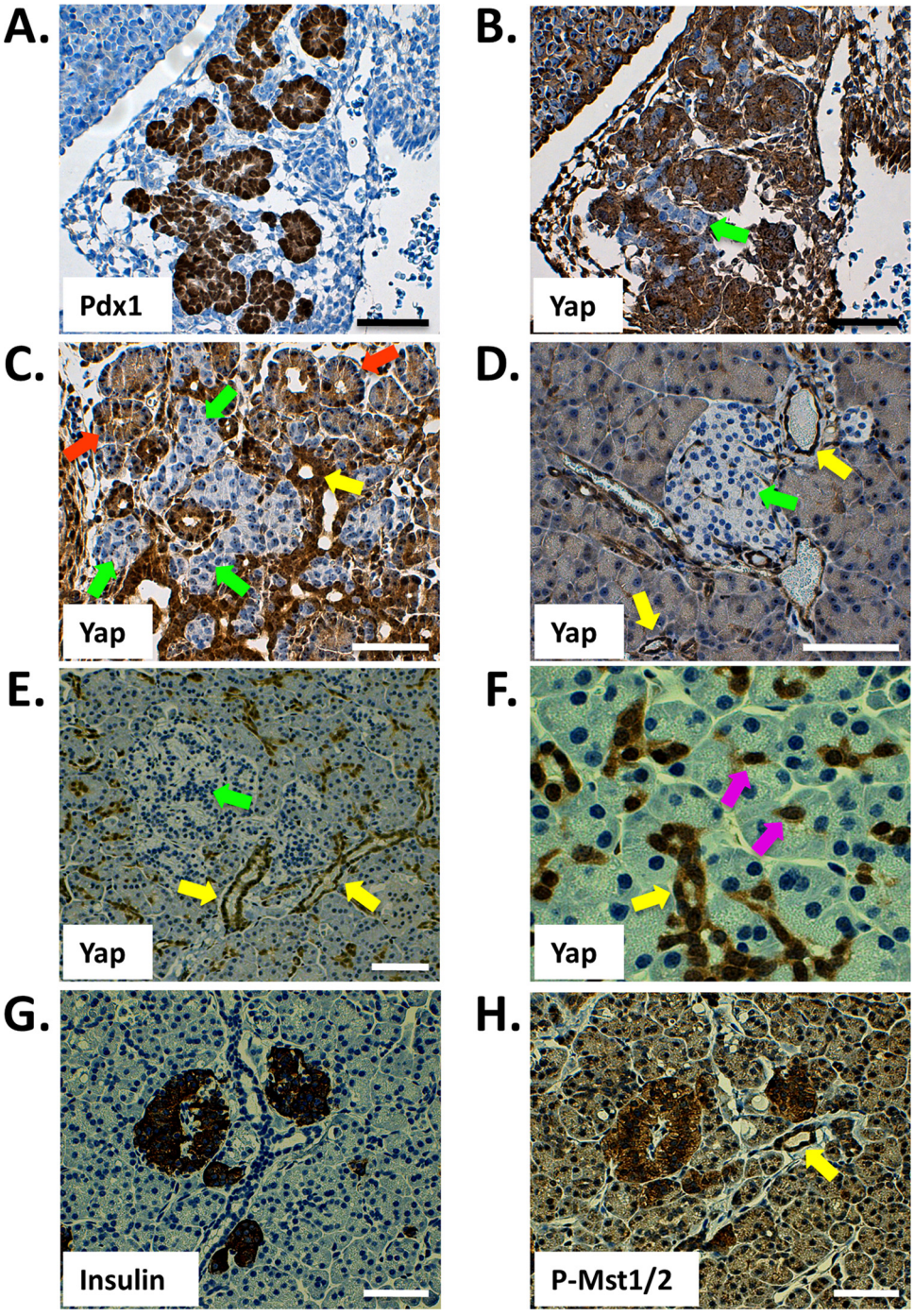

FIG 1 Immunohistochemical detection of Yap and active Mst1/2 in the mammalian pancreas. (A and B) Yap is broadly expressed throughout the Pdx1-positive E12.5 mouse pancreas (sequential sections). (C) Yap expression in the E16.5 pancreas. (D) Yap expression within the pancreas of the adult mouse (at 6 weeks) is largely confined to the ductal network, including terminal duct centroacinar cells, and is undetectable within islets. (E and F) Yap expression in the human pancreas (at 35 years) mirrors that of the mouse, with reactivity observable throughout the ductal network and absent from islets. (G and H) Active Hippo signaling, as determined by phosphorylation-specific Mst1/2 antibody, is present throughout the adult human pancreas. Highest levels of active Hippo signaling are found within islets (sequential sections). Arrows denote prospective or mature cell types, as follows: green, endocrine; orange, acinar; yellow, ducts; violet, centroacinar. Scale bar, 50 μm.

cytoplasmic staining pattern, whereas Yap expression in islets is undetectable. The same pattern of Yap expression is also observed in the human pancreas though expression in acinar cells is weaker (Fig. 1E and F). Based on the known role of Hippo signaling regulating Yap cellular localization and basal protein turnover, we reasoned that active Hippo signaling should display an inverse immunostaining pattern relative to that observed for Yap. As shown in Fig. 1G and H, the active phosphorylated form of Mst1/2

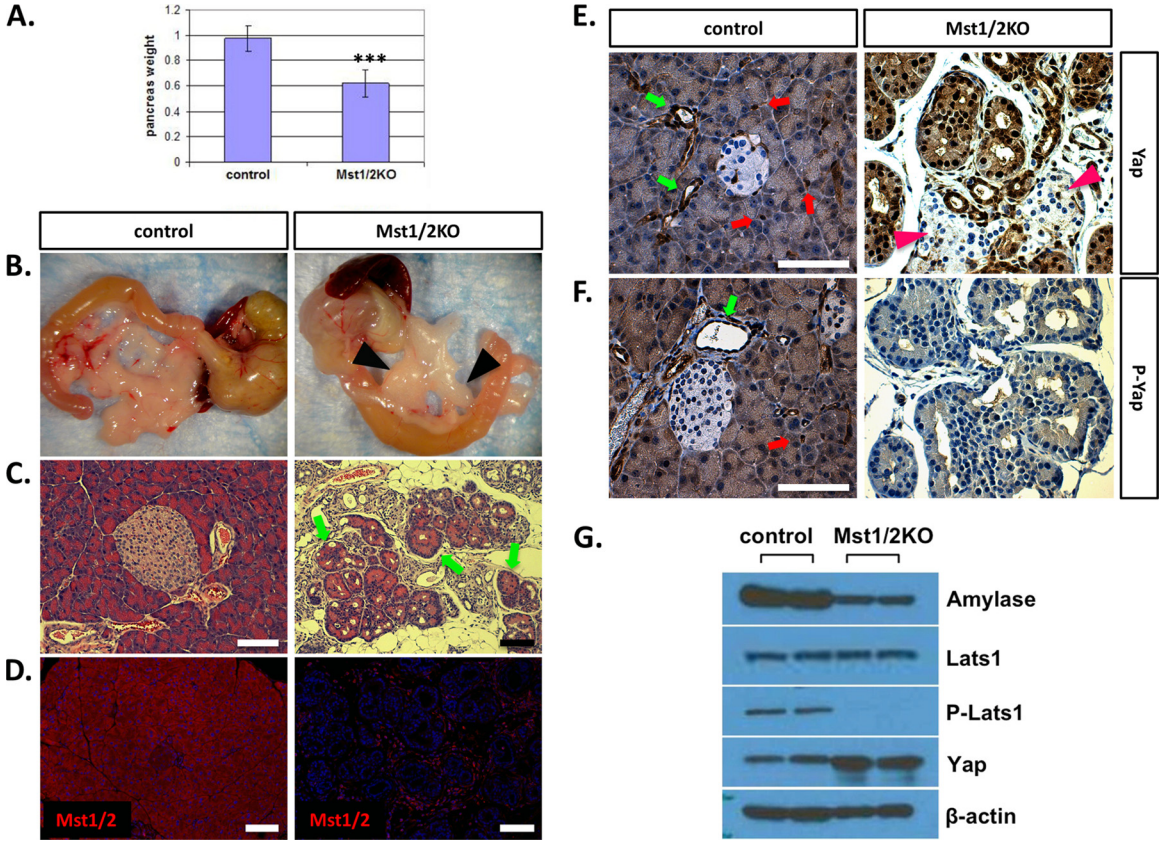

FIG 2 Conditional knockout of Mst1/2 in the mouse pancreas. Floxed Mst1/2 mice were crossed with the Pdx1-Cre strain to delete Mst1/2 throughout the developing pancreas. (A) Relative to controls, pancreas mass, as a percentage of total body weight, was significantly decreased in 6-week-old Mst1/2 KO offspring (***, $P \leq 0.01$). (B) Loss of Mst1/2 leads to an atrophic phenotype characterized by immune cell infiltrate and prominent lymph nodes (arrowheads). (C) Transitional structures, consisting of both acinus-like and duct-like cells, are found throughout the 6-week Mst1/2 KO pancreas (arrows). (D) Efficient Cre-mediated recombination and excision of Mst1/2 as assessed by immunofluorescence detection of Mst1 and Mst2 using a dual-specificity antibody. (E and F) Both total Yap and the Ser127-phosphorylated form of Yap (P-Yap) are detected throughout the normal 6-week exocrine pancreas yet are absent from islet cells (red arrows, centroacinar cells; green arrows, ducts). Yap is nuclear localized and dephosphorylated in the 6-week Mst1/2 KO pancreas. Islands of endocrine cells (arrowheads) remain negative for Yap following Mst1/2 loss. (G) Canonical Hippo signaling regulates Yap phosphorylation and stability in the 6-week pancreas. Scale bar, 50 μm.

(PO_4-Mst1/2) is most readily detectable in pancreatic islets; weaker expression of PO_4-Mst1/2 is observed in acinar and ductal compartments. The specificity of this antibody was excellent, given the complete loss of immunoreactivity on replicate sections treated with phosphatase (see Fig. S1 in the supplemental material). These results suggest that the growth-suppressive Hippo signaling pathway is active within the mammalian pancreas. Furthermore, localization of Yap to the ductal network and centroacinar cells is intriguing, given the role of Yap in maintaining progenitor sources and the fact that the pancreatic ductal epithelium has long been assumed to harbor pancreatic progenitors (2, 3, 13, 23, 30).

Knockout of *Mst1* and *Mst2* in the mouse pancreas. To determine the *in vivo* function of Hippo signaling in the mammalian pancreas, we generated mice with *Mst1* and *Mst2* conditionally inactivated throughout the developing organ by cross to the Pdx1-Cre strain (12, 18). We determined the ratios of observed and expected offspring and found that they were born at the anticipated Mendelian frequency with no observable phenotype. Based on deletion of Mst1/2 in other tissues, we hypothesized that overt pancreas mass would be increased in the knockout offspring (10, 18, 25, 35). As shown in Fig. 2A, pancreas mass was significantly decreased relative to that of wild-type littermate controls. The mutant pancreas was pale white and atrophic relative to that of the controls (Fig. 2B). Histological examination of pancreas tissue from *Mst1* or *Mst2* single deletions indicated no observable difference in architecture relative to controls (data not shown). However, deletion of both *Mst1* and *Mst2* resulted in significantly altered pancreas architecture (Fig. 2C). In contrast to the ordered arrangement of acini, ducts, and islets observed in wild-type offspring, the Mst1/2 knockouts (denoted Mst1/2 KOs) harbored a disorganized arrangement of individual ducts and lacked the rosette-like architecture observed in normal acini (Fig. 2C). Interestingly, structures reminiscent of acinar-ductal transitional units were prominent throughout the Mst1/2 KO pancreas (4, 26). These transitional structures, which mimic the acinar-to-ductal metaplasia observed during pancreatic cancer development, were generally polarized, with nuclei present most frequently along the exterior (Fig. 2C, arrows). Intercalated ducts, which drain exocrine secretions from individual acini, are not visible in the Mst1/2 KOs. In addition, pancreata from Mst1/2 KO mice harbored a robust immune cell infiltrate suggestive of a pancreatitis-like phenotype. Related to this, Mst1/2 KO offspring also presented with

large pancreatic lymph nodes and splenomegaly at dissection (Fig. 2B, arrowheads; also data not shown).

In order to verify the efficiency of Mst1/2 loss following cross to the Pdx1-Cre strain, we utilized a bispecific antibody recognizing conserved residues at the C terminus of both Mst1 and Mst2. As shown in Fig. 2D, expression of Mst1/2 is apparent throughout the wild-type pancreas, detectible in all three major pancreatic cell types. Cellular localization of Mst1/2 was confined mostly to the cytoplasm. In complete contrast, we were unable to detect Mst1/2 protein expression within the epithelium of conditional Mst1/2 KO offspring. There were abundant Mst1/2-expressing cells; however, these were contributed by the extrapancreatic inflammatory infiltrate (Fig. 2D). Extensive loss of Mst1/2 immunoreactivity was also detectible during early stages of pancreas embryogenesis (see Fig. S2 in the supplemental material). These results confirm high-efficiency Cre-mediated recombination and thus Mst1/2 deletion in target offspring.

Hippo signaling regulates Yap stability and cellular localization in the pancreas. In the Hippo signaling pathway, phosphorylation by activated Mst1/2 leads to cytosolic sequestration and proteasome-mediated degradation of Yap. To determine if Mst1/2 loss leads to changes in Yap expression and/or cellular localization, pancreas sections were immunostained for total Yap protein. Whereas Yap is detectible mainly in the ductal system of control mice, its overall expression is increased and detectible throughout the Mst1/2 KO pancreas (Fig. 2E). Strikingly, Yap remains undetectable within pancreatic islet clusters (Fig. 2E, arrowheads). Similar results also hold true for the Yap paralog Taz (see Fig. S3 in the supplemental material).

Yap nuclear localization is generally associated with dephosphorylation at serine-127. To determine whether Mst1/2 deletion leads to Yap dephosphorylation in the pancreas, we immunostained sections with antibody specific for Ser127-phosphorylated Yap. As shown in Fig. 2F, immunoreactivity of PO_4-Yap mirrored that of total Yap in control offspring. In contrast, phosphorylated Yap was nearly undetectable in the Mst1/2 KO offspring (Fig. 2F).

To verify that the results above reflect quantitative changes in Hippo signaling, we examined the phosphorylation status of Hippo pathway components by Western blot analysis. As shown in Fig. 2G, the Mst1/2 phosphorylation target, Lats1, was found nearly exclusively in its dephosphorylated form. Furthermore, total Yap protein levels were found to be elevated following Mst1/2 loss. Altogether, these results confirm that canonical Hippo signaling is functional within the exocrine pancreas. The endocrine compartment, on the other hand, deviates from the norm wherein active Hippo signaling does not directly regulate Yap protein levels.

Defects in pancreatic exocrine and endocrine compartments following Mst1/2 loss. Based on the finding that pancreas mass and tissue architecture are greatly disrupted in the absence of Mst1/2, we wanted to more specifically determine the effects on individual pancreas compartments. Amylase, cytokeratin-19 (CK19), and insulin antibodies specific for the acinar, ductal, and endocrine compartments, respectively, were used to immunostain pancreas sections from adult control or Mst1/2 KO offspring. As shown in Fig. 3A, amylase staining was dramatically altered in the Mst1/2 KOs relative to that observed in controls. Not only did cells within transitional structures stain positive for cytosolic amylase, but some cells first thought to be ductal in phenotype also displayed robust amylase expression (Fig. 3A, arrows). Staining for CK19 (Fig. 3A) indicated duct cell disorganization and mimicked what is commonly observed in acinar-to-ductal metaplasia (12, 26). Histology from offspring of various ages (2 days to 1 year) suggested that the presence of transitional structures occurred early on and persisted throughout the lifetime of the animal (see Fig. S4 in the supplemental material).

Defects in organization within the Mst1/2 KO pancreas are demonstrated further with insulin immunostaining. In contrast to the island-like expression pattern of insulin in wild-type offspring, Mst1/2 KOs displayed highly dispersed islet cells (Fig. 3A). Insulin-positive cells still clustered to form small islets; however, there were numerous single insulin-positive cells found throughout the Mst1/2 KO pancreas. Islet architecture was examined by immunofluorescent localization of insulin and glucagon. Whereas islets from control mice displayed the classical pattern of centrally localized insulin-positive β cells surrounded by a single layer of glucagon-positive α cells, islets from Mst1/2 KO offspring were markedly different (Fig. 3B). Though we observed some normally appearing islets, these were generally smaller (Fig. 3B, bottom). Remarkably, ratios of insulin-positive to glucagon-positive cells remained unchanged between control and Mst1/2 KO offspring (Fig. 3C).

Given the observed changes in islet structure, we asked whether endocrine function was diminished in the Mst1/2 KO pancreas. Normal fed blood glucose levels were mildly higher in Mst1/2 KOs than in control littermates, yet the difference was statistically insignificant (Fig. 3D). Similarly, Mst1/2 KO offspring responded to a fasting glucose challenge equally as well as wild-type offspring (Fig. 3E). It is surprising that defects in islet structure do not translate into changes in endocrine function. Also, this supports the notion that terminal differentiation in islet cells is largely normal in the Mst1/2 KOs.

Mst1 and Mst2 serve as suppressors of proliferation in the mammalian pancreas. Given the stimulatory role of Yap in cell proliferation, we determined relative levels of proliferating cells following Mst1/2 loss. By 6 weeks of age, the majority of pancreatic cells in control offspring are not proliferating, as evidenced by the limited number of cells that incorporate BrdU over a 48-h period (Fig. 4A). In contrast, roughly one-third of the total cells present in the Mst1/2 KO pancreas displayed BrdU incorporation. To more specifically determine rates of proliferation in pancreas cell subcompartments, we determined numbers of replicating amylase-positive (acinar) and CK19-positive (ductal) cells. In both instances roughly one-third of the observed cells incorporated BrdU (Fig. 4A). As shown in Fig. 4B, the location of proliferating cells was generally polarized within transitional structures; most of the Ki67-positive cells were located along the exterior, while the infrequent Ki67-negative cells were located within the interior. Additionally, islet cells were largely Ki67 negative, in agreement with the lack of detectible Yap protein both prior to and following Mst1/2 deletion (data not shown).

Previous studies in the heart demonstrated that Yap-dependent cell proliferation is regulated in part by canonical Wnt/β-catenin signaling (10). Since stabilization of β-catenin has been shown to increase cell proliferation in the pancreas, we next asked if β-catenin is upregulated in the Mst1/2 KO pancreas by using antibody against total β-catenin (11, 28). Whereas β-catenin expression was weak and localized to the plasma membrane in the control pancreas, its expression was dramatically higher in the Mst1/2 KOs (Fig. 4C). Redistribution of β-catenin from the cell

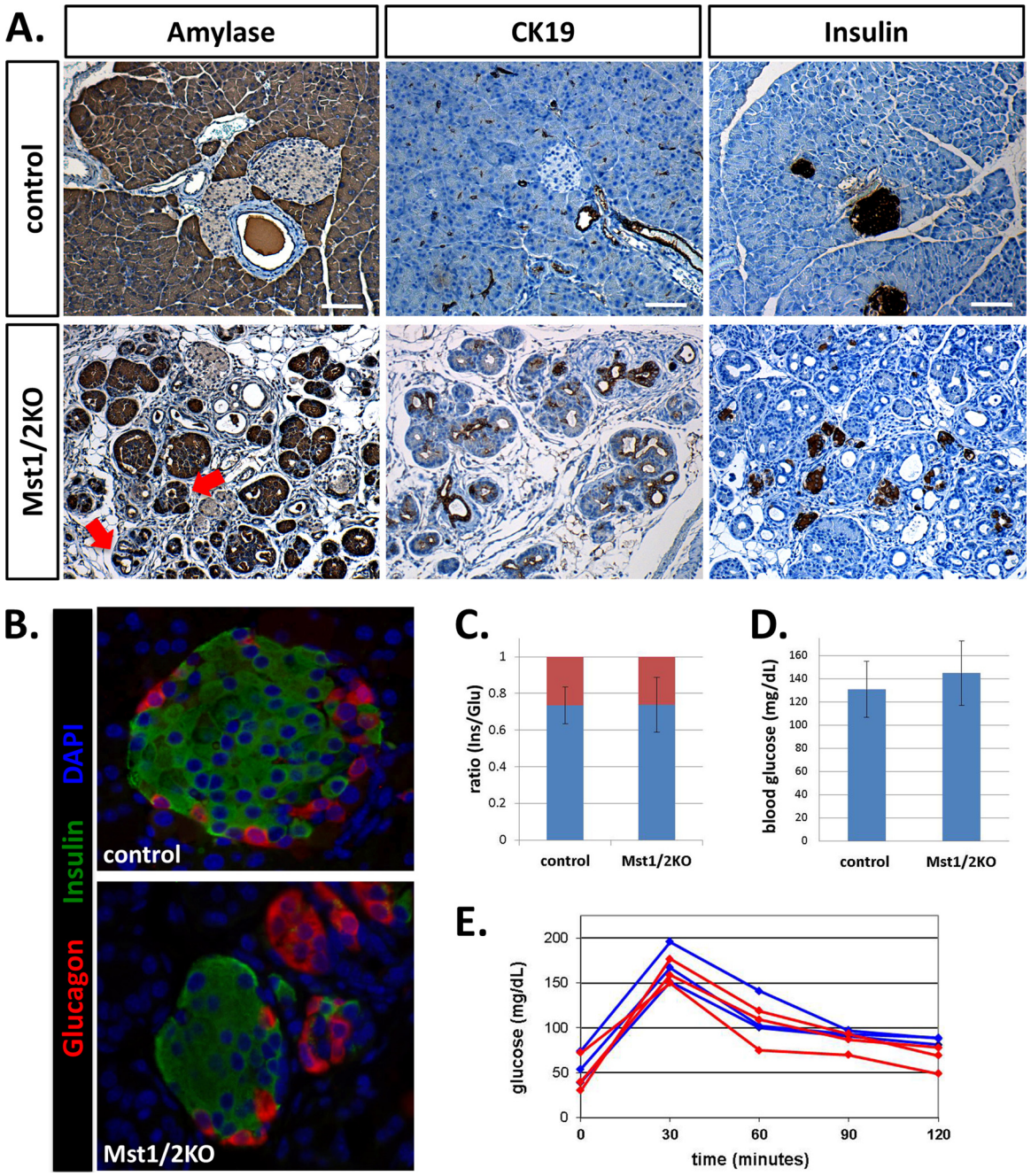

FIG 3 Pancreas-specific knockout of Mst1/2 leads to architectural defects in the exocrine and endocrine compartments yet has negligible effect on glucose homeostasis. (A) Mst1/2 knockout offspring lack the ordered arrangement of acinar cells observed in wild-type controls (both aged 6 weeks). Amylase positivity was detected in cells thought to be duct-like (arrows). Compared to controls, insulin-positive cells are highly dispersed in the Mst1/2 KOs. (B) Endocrine cell populations were characterized using immunofluorescent costaining of insulin and glucagon. Control mice contained normally appearing islets consisting of an insulin-positive interior surrounded by glucagon-positive exterior. Mst1/2 KO offspring harbored smaller islets consisting of cell clusters oftentimes expressing only a single hormone. (C) Ratios of insulin- to glucagon-expressing cells remained unchanged between control and knockout offspring (blue, insulin; red, glucagon). (D) Resting blood glucose levels reveal no significant difference between Mst1/2 KOs and controls ($P = 0.35$). (E) Fasting Mst1/2 KOs respond equally as well as controls following glucose challenge (red, Mst1/2 KO; blue, control). Scale bar, 50 μm.

membrane to the nucleus was evident in the Mst1/2 KOs, which is suggestive of activated transcription (Fig. 4C). Furthermore, immunoreactivity for the dephosphorylated "active" form of β-catenin is detectible in the Mst1/2 KOs and not in control offspring (Fig. 4D). Expression of the Wnt/β-catenin target genes, c-Myc and Tcf1, was found to be substantially elevated in the Mst1/2 KOs (Fig. 4E and F). Interestingly, cells positive for Tcf1 or c-Myc were prominent along the exterior of individual transitional structures, in agreement with those anticipated to be rapidly proliferating (Fig. 4B).

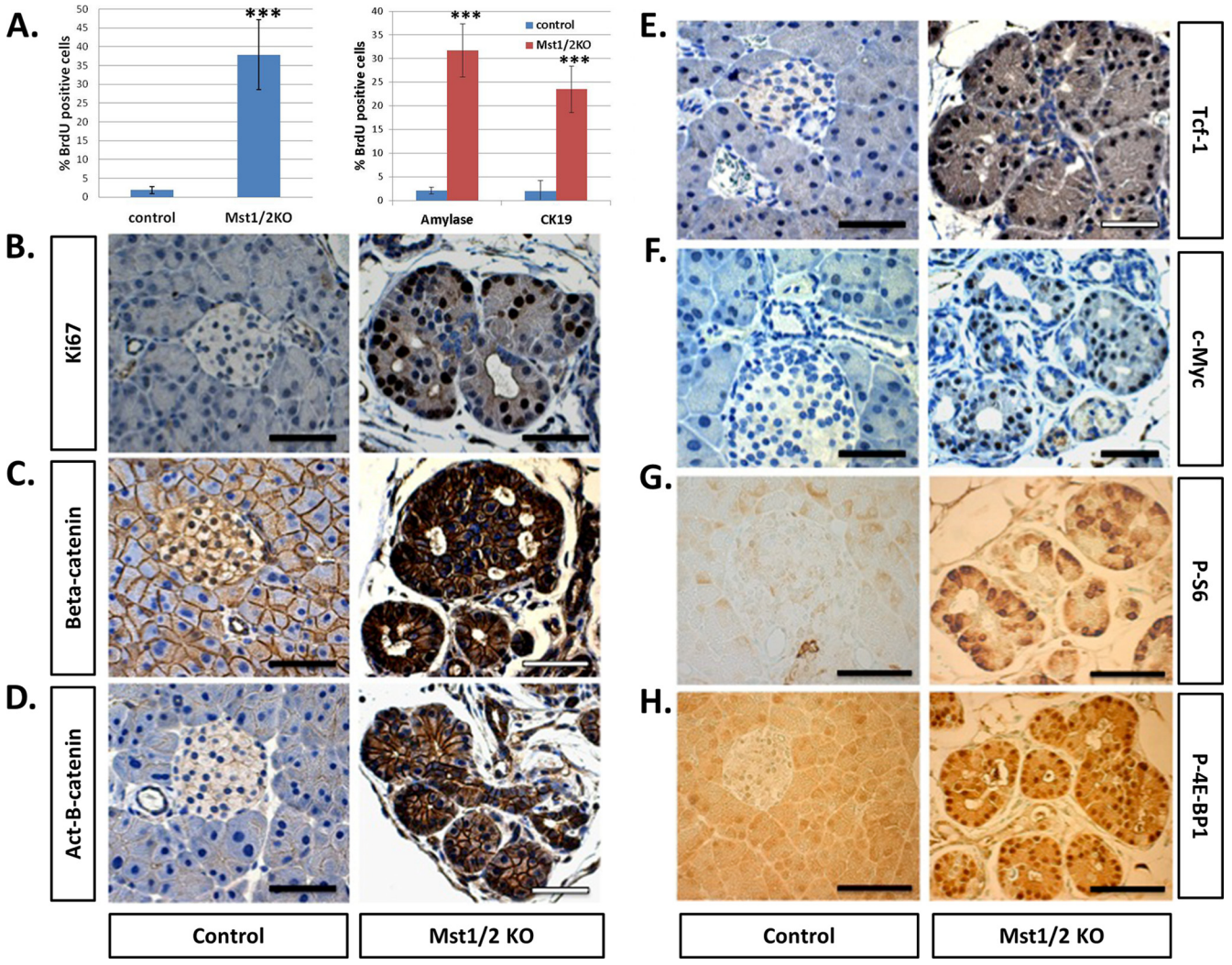

FIG 4 Cell proliferation and signaling through the Wnt/β-catenin and mTOR pathways are robustly increased following pancreas-specific loss of Mst1/2 (6 weeks). (A) Total numbers of actively proliferating cells were quantified based on positivity for BrdU incorporation (left) as well as dual positivity of BrdU/amylase or BrdU/CK19 (right) (***, $P \leq 0.01$). (B) Immunohistochemical detection of Ki67 in controls indicates very few proliferating cells, whereas Ki67-positive cells are readily observed in the Mst1/2 KOs. (C to H) The proproliferative Wnt/β-catenin and mTOR signaling pathways are activated following Mst1/2 loss in the pancreas. Scale bar, 50 μm.

The fact that roughly one-third of cells in the Mst1/2 KO pancreas are actively proliferating suggested that levels of protein synthesis, lipogenesis, and energy expenditure also had to be significantly increased. Mammalian target of rapamycin (mTOR) signaling is a core regulator of growth and energy expenditure, and we analyzed the activation status of this pathway in the pancreas following Mst1/2 loss (17). Phosphorylation of the ribosomal S6 protein and eukaryotic translation initiation factor 4E (eIF4E)-binding protein 1 (4E-BP1) serve as readouts for active signaling through mTOR complex 1 (mTORC1) (17). Whereas phosphorylated S6 and 4E-BP1 are infrequent in the control pancreas, both are easily detectible following Mst1/2 loss (Fig. 4G and H). Levels of total S6 and total 4E-BP1 remain unchanged between controls and Mst1/2 KO offspring (data not shown). Altogether, these results demonstrate that both Wnt/β-catenin and mTOR signaling are activated following Mst1/2 loss in the pancreas and identify mechanisms responsible for the observed increases in cell proliferation. A caveat to these results, however, is the finding that tissue growth is decreased in the Mst1/2 KOs (Fig. 2A).

Autodigestion counteracts cell proliferation within the Mst1/2 KO pancreas. Mst1/2 KOs display a dramatic increase in the number of proliferating cells, yet overall pancreas mass does not increase (Fig. 2A). One explanation for this paradox might be that cells are dying faster than they are produced. To test this possibility, we performed a terminal deoxynucleotidyltransferase-mediated dUTP-biotin nick end labeling (TUNEL) assay to compare the relative levels of apoptotic cells in control and Mst1/2 KO pancreas. To our surprise, TUNEL-positive cells were infrequent and not statistically different from those of controls (see Fig. S5 in the supplemental material). In light of these results, an alternative mechanism for decreased pancreas mass is necrosis, which occurs in pancreatitis, a condition inferred by histologic examination of the Mst1/2 KO pancreas (Fig. 2C). Pancreatitis-like phenotypes have also been observed in mice harboring pancreas-specific de-

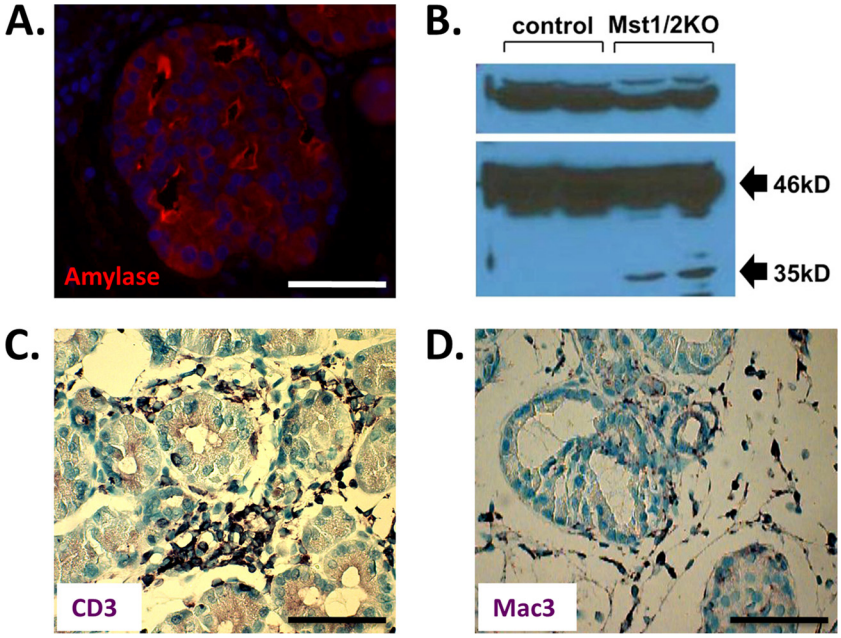

FIG 5 Pancreas autodigestion counteracts cell proliferation. (A) Transitional structures display intense amylase staining along the cell surface of duct-like lumens suggestive of tissue autodigestion. (B) In contrast to controls, 6-week Mst1/2 KOs display intrapancreatic activation of carboxypeptidase A (CPA). Only the 46-kDa proform of CPA is evident in controls, whereas both the proform and the 35-kDa catalytically active form are present in the knockouts. (C and D) Mst1/2 KOs display a robust inflammatory infiltrate consisting of lymphocytes (e.g., $CD3^+$ cells) and macrophage ($Mac3^+$). Scale bar, 50 μm.

letion of the bHLH transcription factor Mist1 or by stabilization of β-catenin during pancreas development (11, 22). Our initial observations suggestive of an autodigestive phenotype stemmed from immunofluorescent analysis of amylase. As shown in Fig. 5A, transitional structures displayed intense amylase reactivity along the plasma membrane of luminal areas. We hypothesized that these regions harbored catalytically active digestive enzymes. Normally, the proforms of these enzymes are extruded from acini into intercalated ducts that merge with the larger exocrine ductal network. However, as intercalated ducts were not observed in the Mst1/2 KO pancreas, these proteins might be released into the tissue, whereby activation may occur. To test this hypothesis, we probed for catalytically active forms of the catabolic enzyme carboxypeptidase A (CPA) in pancreas extracts using Western blot analysis. As demonstrated in Fig. 5B, control pancreas produces only the 46-kDa proform of CPA. In contrast, Mst1/2 KOs displayed a decrease in pro-CPA and presence of the catalytically active 35-kDa form of CPA. The phenotype of the Mst1/2 KO mice thus mimics pancreatitis induced by administration of secretagogues (1). Furthermore, these mice contain a robust immune cell infiltrate. As shown in Fig. 5C and D, lymphocytes and macrophage are common components of the infiltrate. Together, these results suggest that necrosis mediated by autoactivation of digestive enzymes within the mutant Mst1/2 KO pancreas is the major contributor responsible for countering increases in cell proliferation.

Hippo signaling becomes functionally active in the pancreas during the secondary transition. We wanted to determine where changes in pancreas development first become apparent following loss of Mst1/2. Immunofluorescence analysis of the exocrine marker amylase and the epithelial marker E-cadherin was used to compare the morphology of the developing pancreas from E12.5 (primary transition) and E16.5 (secondary transition) embryos. Whereas no discernible difference was observed between controls and Mst1/2 KO offspring at E12.5 (data not shown), defects in development were readily apparent at E16.5 (Fig. 6A). First, we observed a dramatic reduction in the overall expression of amylase, suggesting a defect in exocrine differentiation. The highly E-cadherin-positive trunk region, which gives rise to endocrine and duct cells, did not display an observable morphological difference between Mst1/2 KOs and controls as both harbored a single layer of epithelial cells along the length of the trunk. Upon closer examination of developing Mst1/2 KO acini, we observed cells that were highly nuclear with very little cytoplasm (Fig. 6A, bottom right). Individual Mst1/2 KO acini fail to form the classic rosette-like structure common in controls (Fig. 6A, bottom left). These results led us to assume that negative regulation of Yap must be compromised in the acini of Mst1/2 KO embryos. As shown in Fig. 6B, this was indeed the case, as both the intensity and nuclear localization of Yap within developing acini were greatly increased in the Mst1/2 KOs. In parallel, developing acini from Mst1/2 KOs were highly mitotic, as assessed by BrdU incorporation, whereas those in controls were infrequently mitotic (Fig. 6C). Lastly, cell organization was dramatically different between Mst1/2 KOs and controls. Whereas individual acini in controls displayed luminal expression of the Muc1 glycoprotein, Mst1/2 KOs expressed Muc1 in a disorganized fashion lacking defined lumens (Fig. 6D). These results suggest that Hippo signaling becomes functionally active in pancreas development during the secondary transition where it regulates acinar cell proliferation and tissue organization.

Acinar-ductal transitional structures are produced secondary to a conserved exocrine differentiation program in the Mst1/2 KO pancreas. Hippo signaling is required to maintain progenitor cell populations in the skin, liver, and intestine (18, 24,

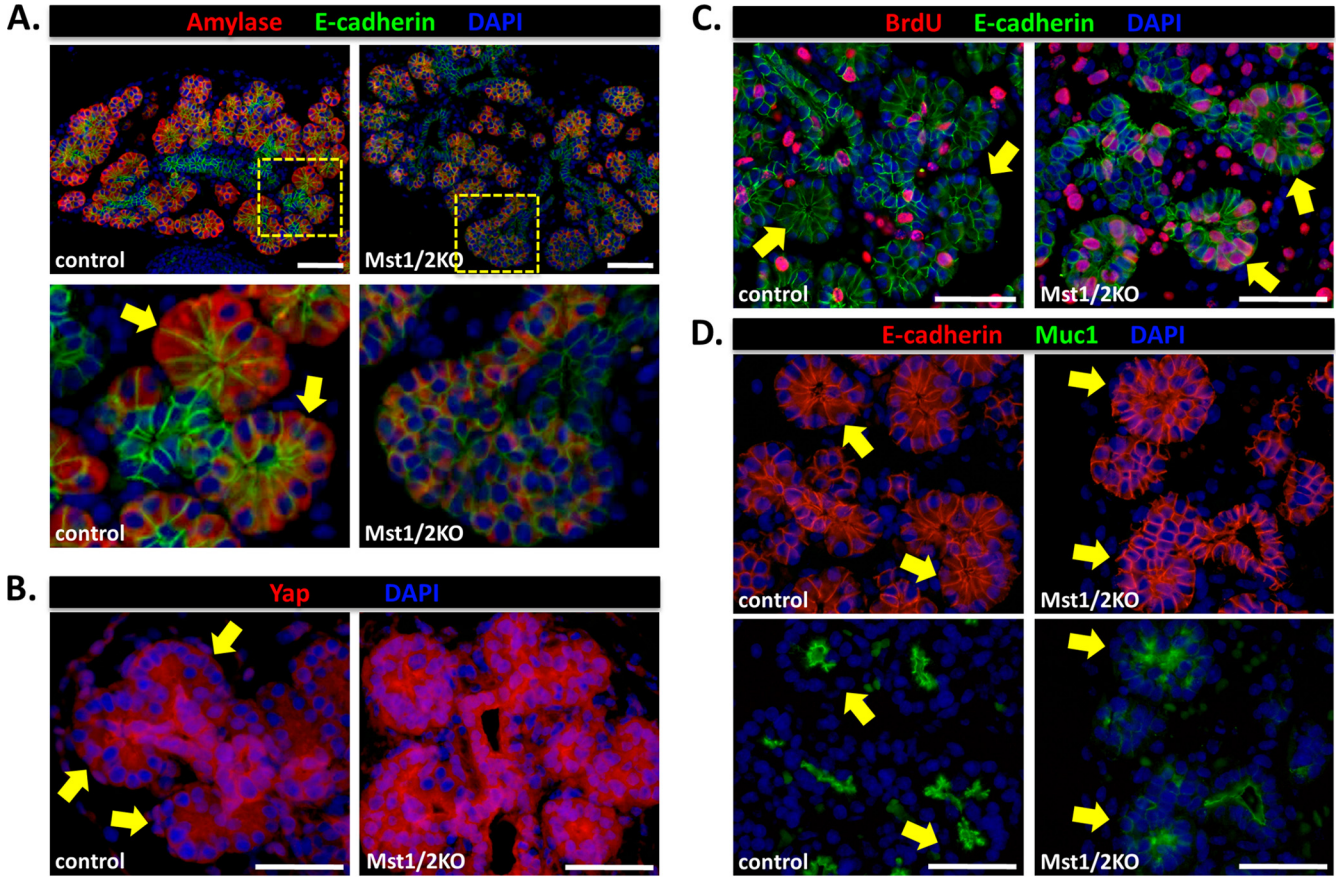

FIG 6 Hippo signaling becomes functionally active in the pancreas during the secondary transition. (A) Immunofluorescence analysis of control and Mst1/2 KO pancreas at E16.5. Loss of Hippo signaling had a trivial effect on the trunk region (E-cadherin) but a dramatic effect on the proacinar tip regions. Amylase staining is dramatically weaker in the Mst1/2 KOs, in line with greatly reduced cytoplasmic content. Tip cells in the knockouts were circular and lacked the "bottle-like" morphology displayed by cells in control mice (bottom panels, arrows). (B) Intense Yap immunoreactivity and nuclear localization within individual acini following Mst1/2 loss. Note the loss of Yap nuclear localization within individual acini of control pancreas. (C) In contrast to the acinar rosettes found in controls, acinar bundles in Mst1/2 KOs contain hyperproliferative cells. (D) Cell organization, as determined by staining with the luminal marker Muc1, is greatly disrupted following Mst1/2 loss. Scale bar, 50 μm.

25, 30, 35). Although the presence of progenitor cells within the adult pancreas remains controversial, cells with the appropriate phenotype are identified in the developing pancreas by expression of the transcriptional regulators Pdx1, Ptf1a, Sox9, and the Notch target gene, Hes1 (15). In particular, during pancreas development the junction between tip cells and trunk cells is thought to harbor a multipotent progenitor population (15, 20, 36). This is significant with regard to the Mst1/2 KO phenotype because Hippo signaling first becomes functionally active within the tip cells (Fig. 6A and B). Thus, defects (i.e., transitional structures) observed in Mst1/2 KO mice may be due to expansion of a pancreas progenitor population. To test this possibility, we completed a time course analysis of Sox9 and Ptf1a expression during pancreas development in the Mst1/2 KO mice. As shown in Fig. 7A, Sox9 and Ptf1a maintained their respective trunk and tip expression patterns during embryonic development (E16.5). Similarly, expression of Mist1, a transcription factor required for acinar function, was found to be highly expressed in developing acinar cells in both control and Mst1/2 KO embryos (Fig. 7B). Together, these results suggest that differentiation within the exocrine pancreas remains intact in the absence of Mst1/2 and, furthermore, does not lead to an expansion of progenitor populations, as shown following Hippo loss within other tissues (18, 24, 25, 30, 35).

Inducible doxycycline-dependent Yap expression has been previously shown to give rise to ductal metaplasia within the mouse pancreas (4). Furthermore, because the observed lesions express Hes1, expansion of a centroacinar cell population was thought to be the precipitating factor. We immunostained sections of 6-week-old Mst1/2 KO pancreas to determine whether individual transitional structures demonstrated reactivity for Hes1 protein. Within individual transitional structures, Hes1 was found to be expressed, however, at a level too infrequent to account for the observed Mst1/2 KO phenotype (Fig. 7C). Additionally, Hes1 expression within both control and Mst1/2 KO E16.5 embryos was limited to rare cells located at the junction of acinar and ductal regions (data not shown) in accordance with previous observations (14). Acinar-ductal transitional structures observed in the Mst1/2 KO pancreas are therefore not likely the result of an expanded centroacinar cell population.

Although developmental differentiation within the Mst1/2 KO pancreas appears to be unaffected, individual transitional structures express both acinar markers (i.e., amylase) and ductal mark-

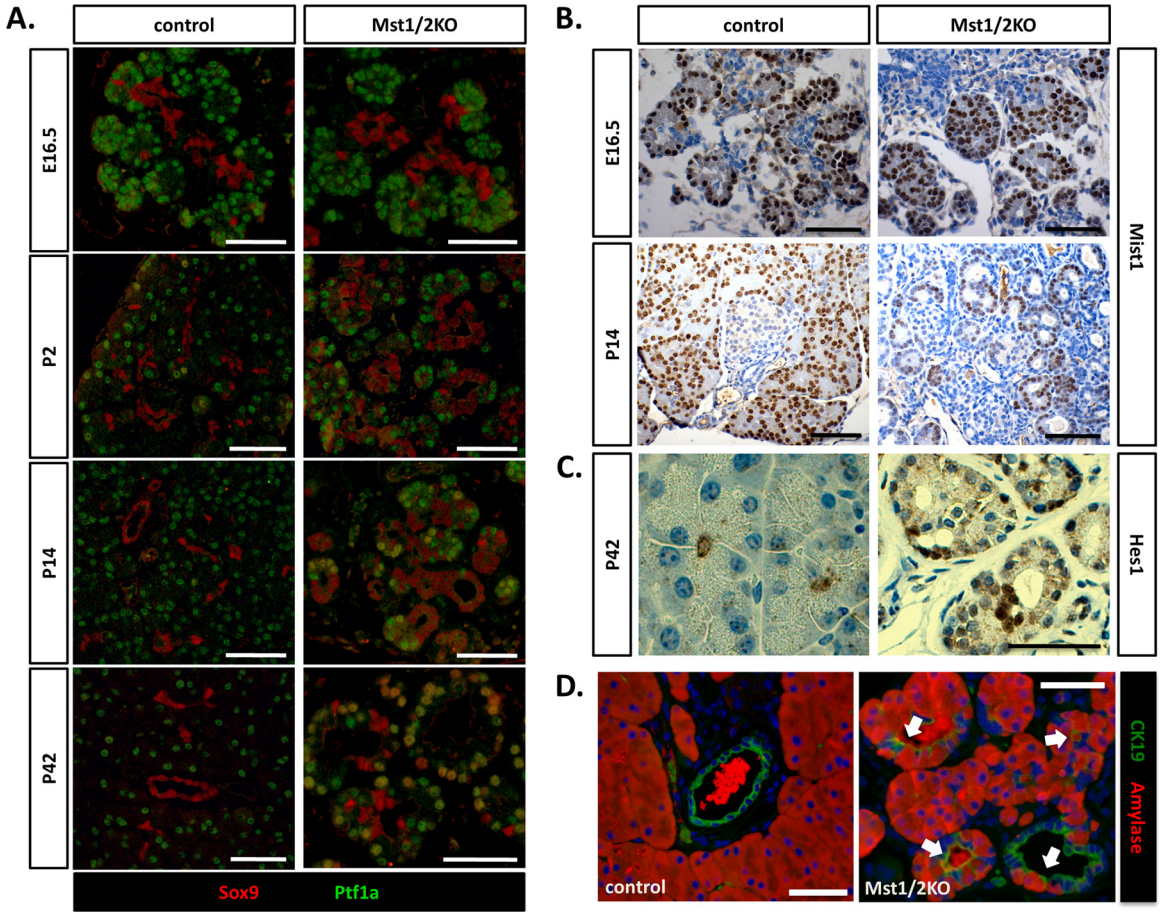

FIG 7 Transitional structures are generated secondary to a normal exocrine differentiation program. (A) Differentiation within the Mst1/2 KO pancreas was monitored over time by analysis of Sox9 and Ptf1a expression. During embryonic pancreas development, Pft1a and Sox9 maintain their respective tip and trunk expression patterns regardless of Mst1/2 presence. Mixed differentiated, Sox9 and Ptf1a doubly positive cells were first observed at 2 weeks postpartum and increased to higher numbers by 6 weeks. (B) Robust expression of Mist1 in developing acini of both control and Mst1/2 KOs suggests normal exocrine differentiation. (C) Analysis of Hes1 expression suggests that transitional structures are not the result of an expanded centroacinar cell population. (D) In line with observation of frequent Sox9/Ptf1a doubly positive cells at 6 weeks, transitional structures contain cells of mixed exocrine status at this stage (arrows, amylase and CK19 copositive). Scale bar, 50 μm.

ers (i.e., CK19), as demonstrated in Fig. 3A. Because transitional structures become apparent by 2 weeks of age (see Fig. S4 in the supplemental material), we hypothesized that exocrine cells at this stage harbor a mixed differentiation status. As shown in the time course presented in Fig. 7A, cells positive for both Sox9 and Ptf1a are first observed at the 2-week time point, and the numbers increase by 6 weeks. To extend this observation one step further, we completed dual immunofluorescence for both amylase and CK19. In agreement with the presence of Sox9/Ptf1a-coexpressing cells, we observed cells doubly positive for CK19 and amylase throughout individual transitional structures (Fig. 7D). Based on timing, our results suggest that the acinar-ductal transitional structures observed in Mst1/2 offspring are likely the result of a pancreatitis-like phenotype secondary to defects in tissue disorganization during development (Fig. 6A to D; see also Fig. S4).

Absence of Yap following endocrine specification in the pancreas. In the pancreas, Hippo signaling is most robust in islets (Fig. 1H); however, following Mst1/2 loss, Yap is not increased within these cells (Fig. 2E). These findings contrast with what is known of the mammalian Hippo signaling pathway, specifically with regard to Mst1/2-dependent phosphorylation and destabilization of Yap (34). To determine at what stage Yap is being downregulated, we took advantage of the fact that endocrine cells become detectible in the embryonic pancreas earlier than functional Hippo signaling (~E10 versus ~E14.5). Importantly, Yap is widely expressed at high levels throughout the embryonic pancreas (Fig. 1A to C). Sequential sections of E12.5 pancreas from wild-type offspring were immunostained for glucagon and Yap. As shown in Fig. 8A, Yap was absent in glucagon-expressing α cells. The same is true of insulin-positive cells; however, fewer insulin-expressing cells are present at this stage of development (data not shown). To determine if this result holds true of endocrine cells produced during the secondary transition, we immunostained sequential sections of E16.5 pancreas for Yap and insulin. As shown in Fig. 8B, Yap expression is undetectable within cells positive for insulin. Remarkably, expression of the Yap paralog, Taz, is also absent from insulin-positive cells, further supporting the conclusion that canonical Hippo signaling does not play a role in the pancreatic endocrine compartment (Fig. 8C). Expression of the transcription factor neurogenin-3 (Ngn3) is crucial for

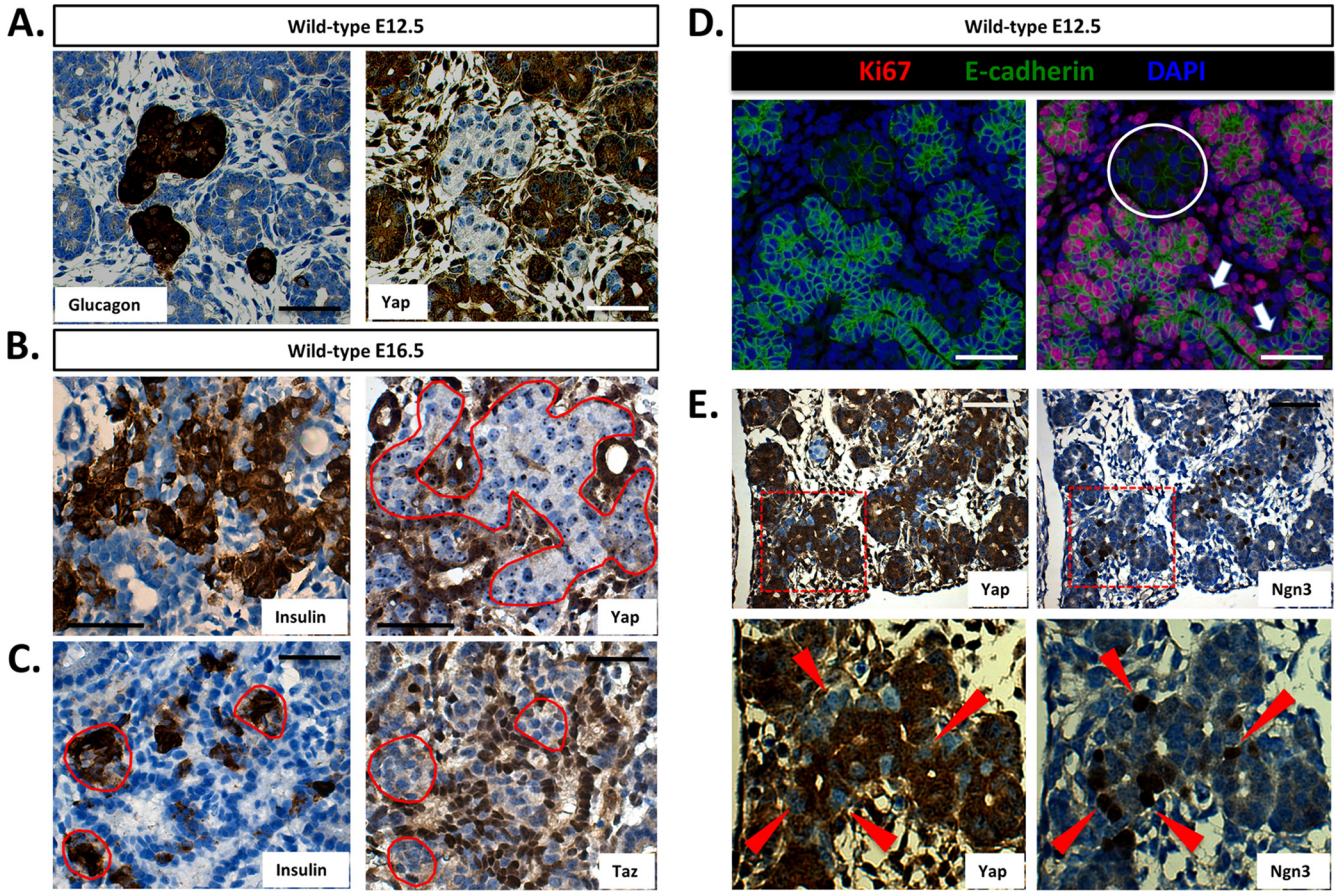

FIG 8 Yap expression is lost following endocrine specification in the pancreas. (A) Yap is undetectable within glucagon-positive endocrine clusters of the E12.5 mouse pancreas (sequential sections). (B and C) Both Yap and Taz are undetectable within insulin-expressing cells in the E16.5 mouse pancreas. (D) Direct correlation between endocrine specification and mitotic potential within the E12.5 mouse pancreas (the circle denotes a single endocrine cluster). Note cells negative for Ki67 along the length of the prospectively Ngn3-studded E-cadherin-positive trunk region (arrows). (E) Inverse correlation between Ngn3 and Yap expression within the E12.5 mouse pancreas (sequential sections; arrowheads represent individual Ngn3-positive/Yap-negative cells). Scale bar, 50 μm.

commitment to the endocrine lineage and is generally associated with cells becoming mitotically quiescent (6, 9, 20). As shown in Fig. 8D, proliferating Ki67-positive cells are absent within E12.5 endocrine clusters. This is in agreement with previous work and suggests a direct correlation between expression of Ngn3 and loss of proliferation (6, 9). Furthermore, as shown in Fig. 8E, we observed substantial overlap between cells positive for Ngn3 and negative for Yap. The Ngn3-positive cells were most frequently located along the trunk epithelium and less at the trunk tips. Together, these results suggest that Yap is lost at the onset of pancreas endocrine specification through a Hippo-independent mechanism, suggesting (i) that Yap expression may demarcate less well differentiated cells and (ii) that the limited proliferation capacity of endocrine cells may be due in part to the absence of Yap.

DISCUSSION

Pancreas development is an intricately orchestrated genetic program regulated by defined sets of transcription factors which ultimately give rise to an organ of correct cell composition and mass. Through inhibition of the transcriptional coactivator, Yap, the Hippo pathway is responsible for regulating organ size. Using loss-of-function analysis in the mouse, we identified a crucial role for Hippo signaling in patterning the developing mammalian pancreas.

Hippo signaling serves as a potent suppressor of proliferation in the mammalian pancreas. Within the adult pancreas, Yap expression is limited to the exocrine compartment, including ductal and acinar cells (Fig. 1D to F). Following Mst1/2 loss, Yap immunoreactivity increases and accumulates within the nucleus of nearly all exocrine cells (Fig. 2E). Phosphorylation of Yap at serine-127 promotes Yap exit from the nucleus, where it is subsequently degraded through a proteasome-dependent mechanism (29, 34). Our results suggest that this situation holds true for the pancreas as following Mst1/2 deletion, Yap is dephosphorylated and accumulates to levels greater than those observed in control mice (Fig. 2F and G). Coincident with Yap nuclear localization, cell proliferation was dramatically increased in the Mst1/2 KOs (Fig. 4A). This was shown to be likely the result of activated Wnt/β-catenin and mTOR signaling. At least one recent report suggests that β-catenin is absolutely required for proliferation increases observed following loss of Hippo signaling in the mouse heart (10). Whether the same holds true in the pancreas remains to be determined. However, several reports suggest that Wnt/β-catenin directly regulates pancreas development and growth through in-

fluence on cell proliferation (11, 28). In both cases mice with stabilized β-catenin harbored increases in overt pancreas mass.

These results are significant because the pancreas ductal epithelium has long been associated with pancreas regenerative potential (2). One recent report utilized an inducible diphtheria toxin model to ablate the pancreatic acinar and endocrine compartments. The remaining ductal epithelium was found to be sufficient for regeneration of the entire organ (5). Whether Hippo signaling was downregulated in the duct cells, thereby allowing Yap-dependent proliferation and organ regeneration, remains a testable question.

Autodigestion leads to decreased pancreas mass in Mst1/2 KOs. A conundrum following deletion of Mst1/2 in the pancreas centered on the lack of increased pancreas mass, as was inferred by ablation of Hippo signaling in other tissues (10, 18, 25). Although roughly one-third of cells were actively cycling in the Mst1/2 KO pancreas, we were surprised to find that overall pancreas mass was less than that observed in controls. These results also contrast with those of murine models containing conditionally stabilized β-catenin, where pancreas mass increases over time (11, 28). This discrepancy may be explained by the prominent tissue disorganization observed in the Mst1/2 KOs, whereas exocrine architecture remained normal following β-catenin stabilization. Why, then, does pancreas mass decrease following Mst1/2 deletion? Our results point to an autodigestive phenotype. Defects are rampant in the Mst1/2 KO pancreas, leading to accumulation of transitional structures containing elements of ductal and acinar lineages. Absence of a continuous ductal system (i.e., lack of intercalated ducts feeding into the larger ductal network) leads to autoactivation of pancreas digestive enzymes and tissue necrosis. Interestingly, at the same time that autodigestion is evident, apoptotic cells are infrequent. This may be explained by the prosurvival influence of Yap signaling (19).

Defects in differentiation status are common in the Mst1/2 KO pancreas. Frequent throughout the Mst1/2 KO pancreas are transitional structures consisting of cells representative of all exocrine cell lineages (acinar, ductal, and centroacinar). However, time course analysis indicated normal exocrine cell differentiation during embryonic development (Fig. 7A and B). Our results suggest that Hippo signaling becomes active in the pancreas during the secondary transition (i.e., E16.5) where it negatively regulates Yap function. In the absence of Mst1/2, we observed high levels of the nucleus-localized form of Yap within developing acini. In parallel, these cells were highly mitotic and lacked the rosette-like organization observed in wild-type acini. Thus, Hippo signaling guides acinar development through negative regulation of proliferation. These results contrast with those observed following Hippo loss in other tissues whereby expansion of progenitor populations occurred (18, 24, 25, 30, 35).

As development progressed in the Mst1/2 KO offspring, we observed a significant change in pancreas architecture beginning between 2 days and 2 weeks postpartum (Fig. 7A and B; see also Fig. S4 in the supplemental material). The pancreas became more ductal and less acinar in phenotype. Although Western blot analysis for intrapancreatic carboxypeptidase-A activation was only completed at the 6-week time point (Fig. 5B), one would assume, based on histology, that pancreatitis-like autodigestion was occurring by 2 weeks of age (see Fig. S4). Simultaneously at this stage of development, cells positive for both Sox9 and Ptf1a become apparent (Fig. 7A). These doubly positive cells are likely copositive for amylase and CK19 and display the hallmarks of acinar-to-ductal metaplasia, a prerequisite to pancreas adenocarcinoma. This raises the possibility that Hippo signaling plays a tumor suppressor role within the pancreas. Though we did not observe tumor development within the Mst1/2 KOs, even at 1 year of age, this does not rule out a role for Hippo signaling in blocking tumor progression (or development). Crossing the conditional Mst1/2 mice with a common progression model of pancreatic cancer would provide a useful model to determine Hippo effects on pancreatic tumorigenesis (12).

Endocrine phenotype following loss of Hippo signaling in the pancreas. Our initial results suggested an inverse correlation between active Hippo signaling and Yap expression (Fig. 1). We were surprised to find that Yap remained undetectable within endocrine cells even in the absence of Mst1/2. These results were further confirmed following cross to the rat insulin promoter-driven Cre recombinase strain which bypasses the observed exocrine phenotype (data not shown). Hippo-independent pathways are therefore thought to be responsible for downregulating Yap expression. Analysis of mouse embryos determined a strict inverse relationship between expression of the endocrine-specifying factor, Ngn3, and expression of Yap (as well as the Yap paralog, Taz). This suggests that Yap is repressed following specification of the endocrine lineage. This is significant because endocrine precursors are generally mitotically quiescent (6, 9, 20). Loss of insulin-producing β cells is the main feature of type 1 diabetes, and replacement therapy by islet transplantation holds curative potential. However, availability of donor islet tissue is rate limiting. Whether reverse genetic engineering, for example, by reintroduction of Yap expression, could stimulate *ex vivo* β-cell proliferation remains an interesting question.

Altogether, these results define a crucial requirement for Hippo signaling in regulating development of the mammalian pancreas. Further research into the role of Hippo signaling during pancreas regeneration holds promise for degenerative disorders, such as diabetes and pancreatitis. Additionally, given Hippo's role in suppressing cell proliferation in the pancreas, future experiments investigating the role of Hippo signaling in pancreatic cancer will determine its translational applicability to this lethal disease.

ACKNOWLEDGMENTS

We thank Elaine Fuchs (Rockefeller University, New York, NY) for the Hes1 antibody. We thank Tao Gao and Ben Stanger (University of Pennsylvania) for sharing results prior to publication. We are grateful to members of the Sarvetnick Lab, particularly Victoria Lao, Kamiya Mehla, and Matthew Wheeler for helpful discussions pertaining to this work. Lastly, critical reviews of the manuscript were kindly provided by Kay-Uwe Wagner and Andy Dudley, both of the University of Nebraska Medical Center.

This work is supported by generous funding from the Kieckhefer Foundation (N.E.S.) and National Institutes of Health (HD060579 to R.L.J.). N.M.G. is supported by an individual NIH postdoctoral fellowship (DK091991).

REFERENCES

1. **Adler G, Hupp T, Kern HF.** 1979. Course and spontaneous regression of acute pancreatitis in the rat. Virchows Arch. A Pathol. Anat. Histol. **382**: 31–47.
2. **Bonner-Weir S, et al.** 2004. The pancreatic ductal epithelium serves as a potential pool of progenitor cells. Pediatr. Diabetes **5**:16–22.
3. **Cai J, et al.** 2010. The Hippo signaling pathway restricts the oncogenic

potential of an intestinal regeneration program. Genes Dev. **24**:2383–2388.
4. **Camargo FD, et al.** 2007. YAP1 increases organ size and expands undifferentiated progenitor cells. Curr. Biol. **17**:2054–2060.
5. **Criscimanna A, et al.** 2011. Duct cells contribute to regeneration of endocrine and acinar cells following pancreatic damage in adult mice. Gastroenterology **141**:1451–1462.
6. **Desgraz R, Herrera PL.** 2009. Pancreatic neurogenin 3-expressing cells are unipotent islet precursors. Development **136**:3567–3574.
7. **Dong J, et al.** 2007. Elucidation of a universal size-control mechanism in *Drosophila* and mammals. Cell **130**:1120–1133.
8. **Gradwohl G, Dierich A, LeMeur M, Guillemot F.** 2000. Neurogenin3 is required for the development of the four endocrine cell lineages of the pancreas. Proc. Natl. Acad. Sci. U. S. A. **97**:1607–1611.
9. **Gu G, Dubauskaite J, Melton DA.** 2002. Direct evidence for the pancreatic lineage: $NGN3^+$ cells are islet progenitors and are distinct from duct progenitors. Development **129**:2447–2457.
10. **Heallen T, et al.** 2011. Hippo pathway inhibits Wnt signaling to restrain cardiomyocyte proliferation and heart size. Science **332**:458–461.
11. **Heiser PW, Lau J, Taketo MM, Herrera PL, Hebrok M.** 2006. Stabilization of beta-catenin impacts pancreas growth. Development **133**:2023–2032.
12. **Hingorani SR, et al.** 2003. Preinvasive and invasive ductal pancreatic cancer and its early detection in the mouse. Cancer Cell **4**:437–450.
13. **Inada A, et al.** 2008. Carbonic anhydrase II-positive pancreatic cells are progenitors for both endocrine and exocrine pancreas after birth. Proc. Natl. Acad. Sci. U. S. A. **105**:19915–19919.
14. **Kopinke D, et al.** 2011. Lineage tracing reveals the dynamic contribution of $Hes1^+$ cells to the developing and adult pancreas. Development **138**:431–441.
15. **Kopp JL, et al.** 2011. Progenitor cell domains in the developing and adult pancreas. Cell Cycle **10**:1921–1927.
16. **Krapp A, et al.** 1998. The bHLH protein PTF1-p48 is essential for the formation of the exocrine and the correct spatial organization of the endocrine pancreas. Genes Dev. **12**:3752–3763.
17. **Laplante M, Sabatini DM.** 2012. mTOR signaling in growth control and disease. Cell **149**:274–293.
18. **Lu L, et al.** 2010. Hippo signaling is a potent in vivo growth and tumor suppressor pathway in the mammalian liver. Proc. Natl. Acad. Sci. U. S. A. **107**:1437–1442.
19. **Pan D.** 2010. The Hippo signaling pathway in development and cancer. Dev. Cell **19**:491–505.
20. **Pan FC, Wright C.** 2011. Pancreas organogenesis: from bud to plexus to gland. Dev. Dyn. **240**:530–565.
21. **Pictet RL, Clark WR, Williams RH, Rutter WJ.** 1972. An ultrastructural analysis of the developing embryonic pancreas. Dev. Biol. **29**:436–467.
22. **Pin CL, Rukstalis JM, Johnson C, Konieczny SF.** 2001. The bHLH transcription factor Mist1 is required to maintain exocrine pancreas cell organization and acinar cell identity. J. Cell Biol. **155**:519–530.
23. **Rovira M, et al.** 2010. Isolation and characterization of centroacinar/terminal ductal progenitor cells in adult mouse pancreas. Proc. Natl. Acad. Sci. U. S. A. **107**:75–80.
24. **Schlegelmilch K, et al.** 2011. Yap1 acts downstream of α-catenin to control epidermal proliferation. Cell **144**:782–795.
25. **Song H, et al.** 2010. Mammalian Mst1 and Mst2 kinases play essential roles in organ size control and tumor suppression. Proc. Natl. Acad. Sci. U. S. A. **107**:1431–1436.
26. **Stanger BZ, et al.** 2005. Pten constrains centroacinar cell expansion and malignant transformation in the pancreas. Cancer Cell **8**:185–195.
27. **Stanger BZ, Tanaka AJ, Melton DA.** 2007. Organ size is limited by the number of embryonic progenitor cells in the pancreas but not the liver. Nature **445**:886–891.
28. **Strom A, et al.** 2007. Unique mechanisms of growth regulation and tumor suppression upon Apc inactivation in the pancreas. Development **134**:2719–2725.
29. **Vassilev A, Kaneko KJ, Shu H, Zhao Y, DePamphilis ML.** 2001. TEAD/TEF transcription factors utilize the activation domain of YAP65, a Src/Yes-associated protein localized in the cytoplasm. Genes Dev. **15**:1229–1241.
30. **Zhang H, Pasolli HA, Fuchs E.** 2011. Yes-associated protein (YAP) transcriptional coactivator functions in balancing growth and differentiation in skin. Proc. Natl. Acad. Sci. U. S. A. **108**:2270–2275.
31. **Zhao B, et al.** 2007. Inactivation of YAP oncoprotein by the Hippo pathway is involved in cell contact inhibition and tissue growth control. Genes Dev. **21**:2747–2761.
32. **Zhao B, et al.** 2008. TEAD mediates YAP-dependent gene induction and growth control. Genes Dev. **22**:1962–1971.
33. **Zhao B, Li L, Lei Q, Guan KL.** 2010. The Hippo-YAP pathway in organ size control and tumorigenesis: an updated version. Genes Dev. **24**:862–874.
34. **Zhao B, Li L, Tumaneng K, Wang CY, Guan KL.** 2010. A coordinated phosphorylation by Lats and CK1 regulates YAP stability through SCF (beta-TRCP). Genes Dev. **24**:72–85.
35. **Zhou D, et al.** 2011. Mst1 and Mst2 protein kinases restrain intestinal stem cell proliferation and colonic tumorigenesis by inhibition of Yes-associated protein (Yap) overabundance. Proc. Natl. Acad. Sci. U. S. A. **108**:E1312–E1320.
36. **Zhou Q, et al.** 2007. A multipotent progenitor domain guides pancreatic organogenesis. Dev. Cell **13**:103–114.